THE AMERICAN SOCIETY OF MECHANICAL ENGINEERS
Three Park Avenue, New York, N.Y. 10016-5990

99-GT-178

Self-Sensing in Fault Tolerant Magnetic Bearings

Dominick Montie
Eric Maslen
Department of Mechanical, Aerospace, and Nuclear Engineering
University of Virginia
Charlottesville, Virginia

ABSTRACT

Several schemes have recently been proposed for achieving either fault tolerance or self-sensing in magnetic bearings. The present work describes the fundamental connection between ability to actuate and ability to sense in a partially failed magnetic bearing system. This relationship is then exploited to construct a self-sensing scheme which operates in the presence of detectable actuator or amplifier faults. Such an approach is advantageous in fault tolerant systems because it reduces or eliminates the need to address potential independent failure mechanisms in sensors and actuators.

Based on a model reference parameter estimation mechanism, the self-sensing scheme is shown to provide acceptable position measurement accuracy and bandwidth under various actuator/amplifier faults which are actuator tolerable. Estimates of increase in noise floor and loss of bandwidth under fault conditions are provided. The issue of estimator convergence under fault conditions is examined in detail with comments on implementation complexity arising from scheduling convergence control on fault state.

INTRODUCTION

Two important issues in the design of magnetic bearings are cost and reliability. In addition to the purchase cost of a magnetic bearing system, it is important to consider the cost of maintenance. The expense of time and resources in repairing a failure (such as bearing coil, amplifier, controller, or sensor failure) may be substantial. Therefore, the ability of a magnetic bearing to be fault tolerant (with respect to failures of one or more of the above) is critical in many applications.

With a self-sensing system, position estimates are obtained by examining the current in the bearing coils, eliminating the need for discrete position sensors. The ability to eliminate the sensors on a magnetic bearing affects cost in both forms, as well as reliability. Self-sensing reduces the initial costs and size of the system/ It also increases reliability by removing a failure susceptible part. While many self-sensing schemes have been demonstrated [3, 6, 7, 8], this technology has not been incorporated into a fault tolerant system.

This combination of fault tolerance and self-sensing is crucial to successful application of magnetic bearings to machinery which is sensitive to cost and down-time, such as most turbomachinery. The potential cost advantages are significant, but more importantly, better reliability will enormously improve acceptance of this technology into common use in production turbomachinery. This is a primary motivation underlying the present work.

In a typical magnetic bearing, such as depicted in Figure 1, the work done by the magnetic field can be described [1] as:

$$w = \frac{1}{2} I^T L I \qquad (1)$$

The force (along the x-axis, for instance) can be derived as:

$$f_x = \frac{\partial w}{\partial x} = \frac{1}{2} I^T \frac{\partial L}{\partial x} I \qquad (2)$$

in which I is assumed to be constant in evaluating virtual work.

As demonstrated in [5], the actuator can generate arbitrary forces in the $x-$ direction if the matrix

Presented at the International Gas Turbine & Aeroengine Congress & Exhibition
Indianapolis, Indiana — June 7–June 10, 1999
This paper has been accepted for publication in the Transactions of the ASME
Discussion of it will be accepted at ASME Headquarters until September 30, 1999

$\partial L/\partial x$ has both positive and negative eigenvalues. In the present work, we demonstrate that the key sensitivity matrix controlling the ability to sense in the $x-$direction is $\partial L^{-1}/\partial x$. The required property is that, again, this matrix should have both positive and negative eigenvalues.

Hence, while a formal proof is not yet developed, there is a strong suggestion that the ability to generate force implies the ability to sense and the ability to sense implies the ability to generate force. On this basis, it is posited that, in any stator axis along which an arbitrary magnetic force can be applied, position sensing can also be achieved. This means that the need for independent fault tolerance mechanisms in the actuators and sensors can be eliminated; for a bearing pole, position sensing is always possible if actuation can be achieved. Whatever scheme is used to preserve the ability to actuate under fault conditions will suffice to preserve the ability to sense.

This paper demonstrates the feasibility of a self-sensing scheme under actuator/coil failures as are typically addressed in a fault tolerant system [5]. In outline, the first section of this paper develops the magnetics model which is used both in a simulation for performance evaluation of the parameter estimator and for derivation of an estimator controller. The parameter estimation scheme is then presented, followed by the techniques used for estimator controller design and construction. Simulation results are then discussed, with emphasis on estimation error, noise, and bandwidth under various fault states. Finally, conclusions and likely avenues of future research are provided.

MAGNETICS MODEL

The magnetic bearing model developed in the paper is based on a typical 8-pole system (see Figure 1), with each coil wound independently and controlled with independent bi-state switching amplifiers. For the purposes of illustration and explanation, some fundamental calculations are examined using a sample 3-pole bearing, with each pole independently wound and spaced 120° apart as indicated in Figure 2.

Begin with the discrete form of Ampere's loop law for the coil fluxes:

$$R\Phi = N_I I \tag{3}$$

To simplify, first assume all of the reluctance is due to the air gap, with no reluctance in the stator or journal, since the relative permeability for many magnetic materials is typically several thousand or greater. Also, assume there are no magnetic non-idealities, such as hysteresis, saturation, or eddy current effects. These assumptions are valid in the linear region of the magnetic material's B-H curve and when the lamination thickness is small relative to reasonable skin depth (order of 0.2 mm).

NOMENCLATURE

symbol	meaning
A_g	cross-sectional area of flux path in air gap
G	force feed-through gain
g	actual average air gap length
g_0	nominal air gap length (room temp., zero speed)
I	vector of bearing coil currents
L	bearing inductance matrix
N_I	magnetic flux linkage matrix
N_V	flux-voltage relationship matrix
n_s	number of coil turns around each pole
R	bearing reluctance matrix
V	vector of coil voltages
w	total energy in a magnetic circuit
v_{ps}	switching amplifier power supply voltage
x	horizontal displacement of the bearing journal, normal to the axis of rotation
y	vertical displacement of the bearing journal, normal to the axis of rotation
z	envelope filter output
α	reciprocal of filter time constant
Δ	diagonal matrix of amplifier duty cycles
Φ	vector of bearing magnetic fluxes
μ_0	magnetic permeability of a vacuum, $4\pi \times 10^{-7}$ Wb/Am
Ω	diagonal matrix of coil resistances
$\dot{(\cdot)}$	time derivative of the quantity $(\cdot)$
$\tilde{(\cdot)}$	estimate of $(\cdot)$

For the 3-pole bearing example, this yields:

$$\begin{bmatrix} r_1 & -r_2 & 0 \\ 0 & r_2 & -r_3 \\ 1 & 1 & 1 \end{bmatrix} \begin{Bmatrix} \phi_1 \\ \phi_2 \\ \phi_3 \end{Bmatrix} = \begin{bmatrix} n_s & -n_s & 0 \\ 0 & n_s & -n_s \\ 0 & 0 & 0 \end{bmatrix} \begin{Bmatrix} i_1 \\ i_2 \\ i_3 \end{Bmatrix}$$

where $r_i = \frac{1}{\mu_0 A_g}(g_0 - x\cos\theta_i - y\sin\theta_i)$ and A_g is taken to be constant over the entire flux path.

Initially, the N_I matrix (and consequently the inductance matrix) has a nullity of 1 since the fluxes in poles 1 and 2 control the flux in the third pole (due to flux conservation). Thus, there is one redundant coil current, from which no flux in the circuit is affected. While this is beneficial in that one coil could fail with negligible loss in performance, the rank deficient inductance matrix means that there is one potentially unstable current state.

Following the method developed in [5], an independent decoupling choke (see Figure 2) is added to the circuit to yield an inductance matrix which is both full rank (of size 3x3 in the example) and decoupled. By attaching each bearing coil in series with windings (of equal turns) around the ring, current vectors orthogonal to the nullity of the original N_I matrix will produce no flux in the ring. In this way, the positive mutual inductances produced by the ring exactly cancel the

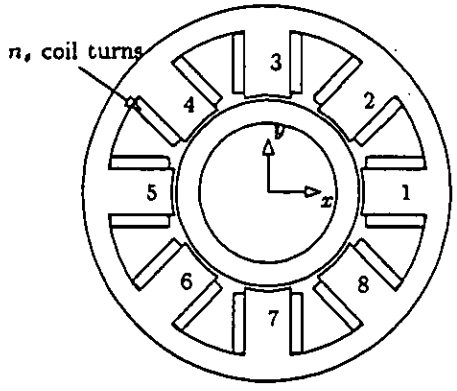

Figure 1: Symmetric 8-pole magnetic actuator.

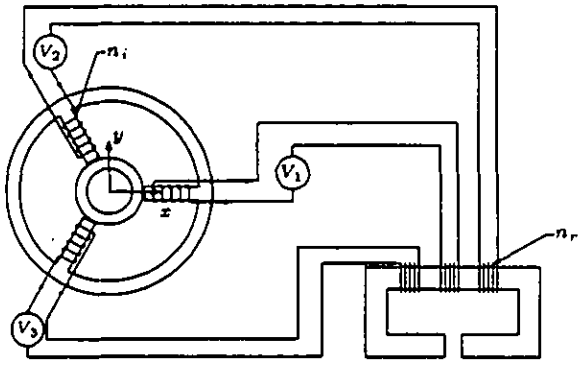

Figure 2: Three pole stator with a decoupling choke.

negative mutual inductances produced in the bearing circuit. The physical parameters of the ring are chosen to produce an inductance matrix that is diagonal under nominal conditions. For the 3-pole example:

$$\begin{bmatrix} r_1 & -r_2 & 0 & 0 \\ 0 & r_2 & -r_3 & 0 \\ 1 & 1 & 1 & 0 \\ 0 & 0 & 0 & r_r \end{bmatrix} \begin{Bmatrix} \phi_1 \\ \phi_2 \\ \phi_3 \\ \phi_r \end{Bmatrix} = \begin{bmatrix} n_s & -n_s & 0 \\ 0 & n_s & -n_s \\ 0 & 0 & 0 \\ n_r & n_r & n_r \end{bmatrix} \begin{Bmatrix} i_1 \\ i_2 \\ i_3 \end{Bmatrix}$$

Applying Faraday's Law and Ohm's Law to the magnetic circuit yields:

$$V = N_V \dot{\Phi} + \Omega I \tag{4}$$

Or, in the example:

$$\begin{Bmatrix} v_1 \\ v_2 \\ v_3 \end{Bmatrix} = \begin{bmatrix} n_s & 0 & 0 & n_r \\ 0 & n_s & 0 & n_r \\ 0 & 0 & n_s & n_r \end{bmatrix} \frac{d}{dt} \begin{Bmatrix} \phi_1 \\ \phi_2 \\ \phi_3 \\ \phi_r \end{Bmatrix} + \begin{bmatrix} \Omega_i & 0 & 0 \\ 0 & \Omega_i & 0 \\ 0 & 0 & \Omega_i \end{bmatrix} \begin{Bmatrix} i_1 \\ i_2 \\ i_3 \end{Bmatrix}$$

Assuming linear magnetics and no eddy currents, the fluxes are computed from (3):

$$\Phi = R^{-1} N_I I \tag{5}$$

From which the example follows:

$$\begin{Bmatrix} \phi_1 \\ \phi_2 \\ \phi_3 \\ \phi_r \end{Bmatrix} = \begin{bmatrix} r_1 & -r_2 & 0 & 0 \\ 0 & r_2 & -r_3 & 0 \\ 1 & 1 & 1 & 0 \\ 0 & 0 & 0 & r_r \end{bmatrix}^{-1} \begin{bmatrix} n_s & -n_s & 0 \\ 0 & n_s & -n_s \\ 0 & 0 & 0 \\ n_r & n_r & n_r \end{bmatrix} \begin{Bmatrix} i_1 \\ i_2 \\ i_3 \end{Bmatrix}$$

When this bearing is centered, $r_1 = r_2 = r_3 = r$:

$$\begin{Bmatrix} \phi_1 \\ \phi_2 \\ \phi_3 \\ \phi_r \end{Bmatrix} = \begin{bmatrix} 2a & -a & -a \\ -a & 2a & -a \\ -a & -a & 2a \\ b & b & b \end{bmatrix} \begin{Bmatrix} i_1 \\ i_2 \\ i_3 \end{Bmatrix} \qquad \begin{aligned} a &= \tfrac{n_s}{3r} \\ b &= \tfrac{n_r}{r_r} \end{aligned}$$

The inductance matrix can then be computed from (5):

$$L \doteq N_V \frac{\partial \Phi}{\partial I} = N_V R^{-1} N_I \tag{6}$$

From the previous derivation, L for the 3-pole bearing example becomes:

$$\begin{aligned} L &= \begin{bmatrix} n_s & 0 & 0 & n_r \\ 0 & n_s & 0 & n_r \\ 0 & 0 & n_s & n_r \end{bmatrix} \begin{bmatrix} 2a & -a & -a \\ -a & 2a & -a \\ -a & -a & 2a \\ b & b & b \end{bmatrix} \\ &= \begin{bmatrix} 2an_s + bn_r & -an_s + bn_r & -an_s + bn_r \\ -an_s + bn_r & 2an_s + bn_r & -an_s + bn_r \\ -an_s + bn_r & -an_s + bn_r & 2an_s + bn_r \end{bmatrix} \end{aligned}$$

Each off-diagonal term, when equated to zero (to yield a diagonal inductance matrix), produces the relationship:

$$bn_r = an_s \Longrightarrow \frac{n_r^2}{r_r} = \frac{n_s^2}{3r} \tag{7}$$

which determines the necessary geometry of the decoupling choke to make (7) valid. For a general symmetric p–pole stator, this relationship is $n_r^2/r_r = n_s^2/pr$. Using this design constraint for the decoupling choke produces a diagonal inductance matrix for $x = y = 0$: $L = \mathrm{diag}(n_s/r)$.

Combining equations (4) and (5) yields:

$$\begin{aligned} V &= N_V \frac{d}{dt}(R^{-1} N_I I) + \Omega I \\ &= L\dot{I} + \dot{L} I + \Omega I \end{aligned} \tag{8}$$

The dynamic behavior of the actuator is governed by:

$$\dot{I} = L^{-1}\left(V - \left[\dot{L} + \Omega\right] I\right) \tag{9}$$

in which the flux and current are nonlinear functions of x, y, g, and V. L is invertible because of the addition of the decoupling choke.

AMPLIFIER SIMULATION

Magnetic bearings typically use switching power amplifiers in a transconductance mode. These amplifiers

compare a requested current to their actual output current and select the output voltage accordingly. In a bi–state amplifier, this output voltage is either $+v_{ps}$ or $-v_{ps}$: choosing $+v_{ps}$ will increase the coil current. In a tri–state amplifier, a third output condition of 0 volts (coil shorted) is added. A specific limitation of the present work is that it assumes bi–state operation even though commercial practice has very broadly adopted tri–state amplifiers because of their lower power losses and acoustic noise emission. The self–sensing scheme presented here does not fundamentally require bi–state operation, but the interrogation signal is much stronger and easier to process in bi–state than in tri–state: experimental results with tri–state so far have been poor.

The actual amplifier scheme used in the present simulation is a time delay algorithm[4]: a comparator determines a desired output state based on the difference between the reference and measured currents. This output state is then implemented a short time later (13 microseconds in the simulation). The result is stable current control with a switching limit cycle with overall period of 52 microseconds: about 20 kHz. Similar behavior would be obtained with any of a number of other switching algorithms.

The target currents determine the force produced by the actuator. Meeker[5] provides a thorough coverage of this in both the nominal case and when the actuator has a fault. For the simulations here, the target currents were held at a nominal bias condition, so the effect of target current dynamic behavior was not examined. For the single magnet case, Noh[7] provides an extensive discussion of the effect of dynamic current reference.

FAULT CONDITIONS

The fault mechanism addressed in this work is an open circuit at any point in the series connection of amplifier, wiring, and coil. Such a fault includes fuse burnout, amplifier device burnout (in the open condition), coil wire burnout, and connector failure. It does not consider the shorted coil scenario or other short failures as in the power amplifier. In open circuit failures, the coil current goes to zero: for short failures, the coil voltage goes to zero and the current is driven by stator flux variation. While either mechanism is possible, industrial experience suggests that the open coil scenario is more commonly encountered.

Modeling an open coil failure is simple: the current in the failed coil is forced to zero. The actual coil voltage has no effect on the dynamics of the simulation so it can be assumed zero. In (9), this means that failure of coil i is equivalent to removing the i^{th} row and column of each of the matrices.

PARAMETER ESTIMATION SCHEME

Information about the gap reluctances, and hence the rotor position, is most richly embedded in the time rate

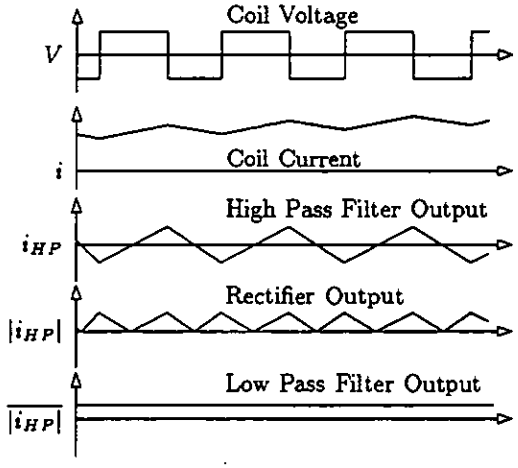

Figure 3: Sequence of signals in envelope filter.

of change of the coil currents. Following [7], a set of filters is used to approximate the magnitudes of the slopes of each current. This is achieved with a high-pass filter (to remove the low-frequency components of the current), followed by a rectifier and a low-pass filter (to demodulate the amplitude of the signal). A simplified model of the action of the envelope filter is a low pass filter acting on $|\dot{I}|$, with a cutoff frequency of about 2kHz: Figure 3 illustrates the sequence of signal operations.

The output approximates the magnitude of the current slope up to the bandwidth of the filter. The filter output is, however, *also* a function of the amplifier duty cycle (directly related to actuator force slew rate). Consequently, it is undesirable to use this signal directly as a measure of gap length.

Instead, a parameter estimation scheme uses this information (which is monotonic in gap length[7]) to estimate the actual gap length independently of the amplifier duty cycle. An analog circuit simulation of the magnetics is driven by the actual coil voltages. The air gaps (x, y, g) of the simulation are to be determined and form the output of the parameter estimator.

The simulation produces a set of coil currents which, if the simulation air gaps are correct, should match the actual currents. The simulation currents are filtered in the same manner as the actual currents and the error between the two filtered sets of currents is applied to a controller which attempts to determine the estimated position, as depicted in Figure 4. If the loop closed by this controller is stable, then the error should converge to zero which is equivalent to the estimated gaps converging to the actual gaps. Noh[7] provides a very extensive discussion of this approach for the problem of estimating a single air gap.

PLANT LINEARIZATION

The first step in developing this controller is to extract a linearized model for the dynamics of the error between the actual filtered currents and the output of the

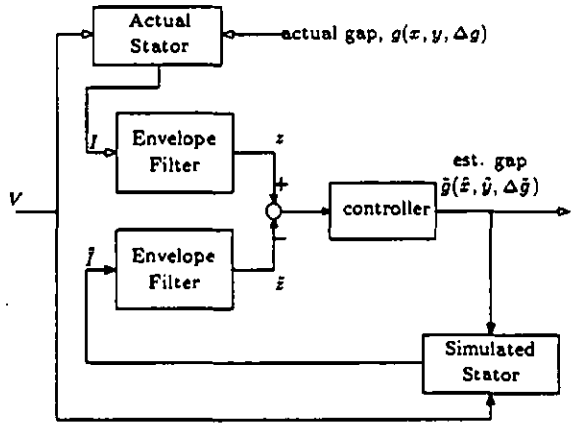

Figure 4: Parameter estimation scheme.

simulation. The plant magnetics are described by (9):

$$\begin{aligned} \dot{I} &= A(x,y,g)I + B(x,y,g)V \\ A(x,y,g) &\doteq -L^{-1}\left[\frac{dL}{dt} + \Omega\right] \\ B(x,y,g) &\doteq L^{-1} \end{aligned}$$

and the simulation dynamics are described by:

$$\dot{\tilde{I}} = A(\tilde{x},\tilde{y},\tilde{g})\tilde{I} + B(\tilde{x},\tilde{y},\tilde{g})V \tag{10}$$

Following[7], the envelope filters are modeled as:

$$\begin{aligned} \dot{o} &= -\alpha a + \alpha|\dot{I}| \\ z &= 4\Delta(I-\Delta)a \end{aligned} \tag{11}$$

The nominal duty cycle of the amplifiers in two–state mode is 0.5. Thus, at the nominal duty cycle, z is a low pass version of $|\dot{I}|$. A similar equation can be written for the output filters acting on the simulation.

To eliminate the nonlinearity of the output equation in (11), expand in a Taylor's series as

$$\begin{aligned} z &= 4\Delta_0(I-\Delta_0)a_0 + 4(\Delta-\Delta_0)(I-2\Delta_0)a_0 \\ &\quad -4(\Delta-\Delta_0)^2 a_0 \end{aligned}$$

Noting that $\Delta_0 = \mathrm{diag}(0.5)$ and $o_0 = |\dot{I}|_0$, this is

$$z = a - 4(\Delta-\Delta_0)^2|\dot{I}|_0$$

The last term in this equation is a mess and not particularly easily measured, so treat it as an unknown excitation:

$$Gf \doteq -4(\Delta-\Delta_0)^2|\dot{I}|_0 \tag{12}$$

in which G is a property of the actuator and f is controlled by the switching sequence. The estimator will be subject to the same f, but with an estimated gain $\tilde{G}$.

After a little simple algebra, the intermediate variable a is eliminated to leave (for the actual actuator)

$$\dot{z} = -\alpha z + \alpha|\dot{I}| + G(\alpha f + \dot{f}) \tag{13}$$

and for the simulation,

$$\dot{\tilde{z}} = -\alpha\tilde{z} + \alpha|\dot{\tilde{I}}| + \tilde{G}(\alpha f + \dot{f}) \tag{14}$$

In order to reflect the effects of x, y, and g on these dynamics, expand $|\dot{I}|$. From (9), a first order Taylor's series expansion about $x = y = g - g_0 = 0$ gives

$$\begin{aligned} \dot{I} &\approx L_0^{-1}(V-\Omega I) \\ &\quad -L_0^{-1}\left(\frac{dL}{dx}x + \frac{dL}{dy}y + \frac{dL}{dg}\Delta g\right)L_0^{-1}(V-\Omega I) \\ &\quad -L_0^{-1}\left(\frac{dL}{dx}\dot{x} + \frac{dL}{dy}\dot{y} + \frac{dL}{dg}\dot{g}\right)I \end{aligned}$$

Assume that the amplifier voltage is much larger than the resistive drop due to coil resistance: $V \gg \Omega I$. Further, assume that the velocity induced term (the last term) is negligible. With this,

$$\dot{I} \approx L_0^{-1}\left[L_0 - \left.\frac{dL}{dx}\right|_0 x - \left.\frac{dL}{dy}\right|_0 y - \left.\frac{dL}{dg}\right|_0 \Delta g\right] L_0^{-1}V \tag{15}$$

Define the coefficients of this series as

$$K_0 \doteq L_0^{-1} \tag{16}$$

$$K_x \doteq -L^{-1}\frac{dL}{dx}L^{-1}\Big|_0 \tag{17}$$

$$K_y \doteq -L^{-1}\frac{dL}{dy}L^{-1}\Big|_0 \tag{18}$$

$$K_g \doteq -L^{-1}\frac{dL}{dg}L^{-1}\Big|_0 \tag{19}$$

so that

$$\dot{I} \approx K_0 V + K_x V x + K_y V y + K_g V(g-g_0) \tag{20}$$

and

$$|\dot{I}| \approx |K_0 V + K_x V x + K_y V y + K_g V(g-g_0)| \tag{21}$$

This absolute value function makes analytic evaluation somewhat difficult. However, if $K_0 V$ is enough bigger than the other terms (which it generally is) then this expression can be expanded in a series of the form

$$|\dot{I}| \approx k_0' + k_x' x + k_y' y + k_g'(g-g_0) \tag{22}$$

where

$$\begin{aligned} k_0'(V) &\doteq |K_0 V| \\ k_x'(V) &\doteq \frac{|K_0 V + K_x V x| - k_0}{x} \\ k_y'(V) &\doteq \frac{|K_0 V + K_y V y| - k_0}{y} \\ k_y'(V) &\doteq \frac{|K_0 V + K_g V(g-g_0)| - k_0}{g-g_0} \end{aligned}$$

The k_j are dependent upon the instantaneous collection of coil voltages, V. However, given that V lies in the set $v_i = \pm v_{ps}$ and the voltage states switch very

rapidly and more or less independently, it may make sense to evaluate the *expected value* of these expressions by averaging over all possible voltage combinations:

$$k_j = \mathcal{E}(k_j) = \frac{1}{2^p}\sum_{i=1}^{2^p} k_j'(v_i) \tag{23}$$

and to assume that the filter dynamics (which are low pass filtered) are governed by these expected values. The expected values of k_j turn out to be the diagonal elements of the corresponding K_j scaled by the power supply voltage and are independent of the displacement (x, y, or g) selected for evaluation of the derivatives as long as these displacements are less than g:

$$k_j = \mathrm{diag}(K_j)v_p s \tag{24}$$

The net result of all of this manipulation is a linearized model for the filter output as driven by the displacements which are to be estimated:

$$\dot{z} = -\alpha z + \alpha k_0 + \alpha\,[k_x\ k_y\ k_g]\begin{Bmatrix} x \\ y \\ g - g_0 \end{Bmatrix} + G(\alpha f + \dot{f})$$

for the actual stator and

$$\dot{\tilde{z}} = -\alpha \tilde{z} + \alpha k_0 + \alpha\,[k_x\ k_y\ k_g]\begin{Bmatrix} \tilde{x} \\ \tilde{y} \\ \tilde{g} - g_0 \end{Bmatrix} + \tilde{G}(\alpha f + \dot{f})$$

for the simulated stator.

The objective of the controller is to drive the error between z and $\tilde{z}$ to zero, so define error coordinates $e \doteq z - \tilde{z}$ to obtain

$$\dot{e} = -\alpha e + \alpha\,[k_x\ k_y\ k_g]\begin{Bmatrix} x - \tilde{x} \\ y - \tilde{y} \\ g - \tilde{g} \end{Bmatrix} + (G - \tilde{G})(\alpha f + \dot{f}) \tag{25}$$

In the limit as $e \to 0$, $\tilde{G} \to G$ so that the influence of f will be negligible: this is largely the purpose of using a parameter estimator.

Each error state e is accessible so state feedback can be employed directly in regulating e. The result is a MIMO LQR controller that minimizes the error over all voltage switch states and under various fault conditions by converging the values of the estimated inputs to those of the actual plant inputs.

CONTROLLER CONSTRUCTION

The linear error dynamic model presented in (25) contains a number of external inputs which are essentially unknown: x, y, g, and f. A simplistic approach to designing a controller with these signals present is to assume that they are zero mean, random, Gaussian distributed signals. As such, it is not possible to predict future values of these signals even if the entire time history up to the present is known. Therefore, the controller is derived without regard to these signals and the plant model takes the simpler form:

$$\dot{e} = -\alpha e - \alpha\,[k_x\ k_y\ k_g]\begin{Bmatrix} \tilde{x} \\ \tilde{y} \\ \tilde{g} \end{Bmatrix} \tag{26}$$

The control variables are the estimated rotor position ($\tilde{x}$, $\tilde{y}$) and mean radial air gap ($\tilde{g}$). A suitable cost function for construction of a linear quadratic regulator solution[2] weights the states against the control "effort".

The parameters of this model (k_x, k_y, and k_g) are dependent upon the fault state. Potentially, it will be necessary to derive a different controller for each possible fault state. However, as presented in the following section, a single controller derived at nominal no–fault conditions will provide adequate tracking even for multiple coil failure modes.

To demonstrate construction of the controller, return to the 3–pole example for which the plant model becomes:

$$\dot{e} = -\alpha e - \alpha\,[k_x\ k_y\ k_g]\begin{Bmatrix} \tilde{x} \\ \tilde{y} \\ \tilde{g} \end{Bmatrix}$$

$$\begin{Bmatrix} y_1 \\ y_2 \\ y_3 \\ y_4 \\ y_5 \\ y_6 \end{Bmatrix} = \begin{bmatrix} \frac{1}{\epsilon_1} & 0 & 0 \\ 0 & \frac{1}{\epsilon_2} & 0 \\ 0 & 0 & \frac{1}{\epsilon_3} \\ 0 & 0 & 0 \\ 0 & 0 & 0 \\ 0 & 0 & 0 \end{bmatrix} e + \begin{bmatrix} 0 & 0 & 0 \\ 0 & 0 & 0 \\ 0 & 0 & 0 \\ \frac{1}{\delta_x} & 0 & 0 \\ 0 & \frac{1}{\delta_y} & 0 \\ 0 & 0 & \frac{1}{\delta_g} \end{bmatrix} \begin{Bmatrix} \tilde{x} \\ \tilde{y} \\ \tilde{g} \end{Bmatrix} \tag{27}$$

where $\alpha = 4\pi \times 10^3$ and K is a scaling constant used for controller calibration of outputs $\tilde{x}, \tilde{y}$, and $\tilde{g}$. The scalings ϵ_i are identical filter error magnitudes and δ_i are the maximum controller output magnitudes used in the cost functions y_{pi}. As discussed in [7], stability of the estimator sets an upper bound on the ratio of δ_i/ϵ_i while convergence rate sets a lower bound. In the present work, this ratio was selected to be as large as possible without encountering instability in the simulation. The ϵ_i are chosen to be very small (0.01 volts in the simulation) while the δ_i, were quite large (100 meters in the simulation).

The parameter estimation controller is computed as a linear quadratic regulator by formulating an algebraic Ricatti equation and solving for the resulting state feedback matrix[2] so that

$$\begin{Bmatrix} \tilde{x} \\ \tilde{y} \\ \tilde{g} \end{Bmatrix} = Ke \tag{28}$$

SIMULATION RESULTS

The relevant parameters of the magnetic bearing we simulated were $g_0 = 1.0$ mm, $A_g = 4.91$ cm^2, and

Table 1: Sensing performance under various fault scenarios.

Run	Coils Failed	X_{mag}	X_{phase}	X_{rms}^{error}	Y_{mag}	Y_{phase}	Y_{rms}^{error}
1	0	46.4 μm	$-3.8°$	0.7 μm	46.4 μm	$-3.8°$	0.7 μm
2	1, X-axis	43.9 μm	$-2.7°$	3.3 μm	46.1 μm	$-2.1°$	0.7 μm
3	1, Y-axis	46.1 μm	$-2.1°$	0.7 μm	43.9 μm	$-2.7°$	3.3 μm
4	1, Off-axis	47.7 μm	$-3.4°$	9.5 μm	47.7 μm	$-3.4°$	9.5 μm
5	2, Off-axis, adj.	46.9 μm	$-3.1°$	2.8 μm	47.0 μm	$-3.1°$	10.0 μm

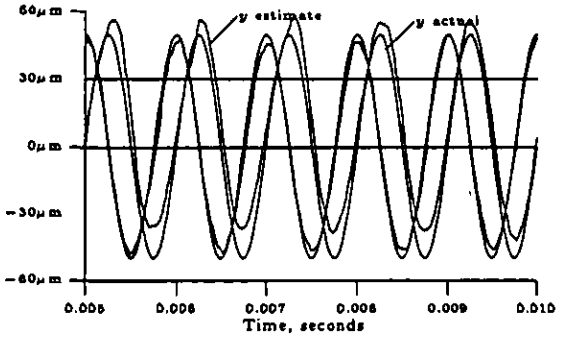

Figure 5: Simulation results for run 5: two coils failed.

$n_s = 200$. To remove the effect of turn-on transients, the tracking controller is suppressed for 2 ms. At 2 ms, the estimator is enabled, causing the controller to produce transients of its own as it begins tracking the actual filter output from the nominal filter output at zero estimated displacement. Therefore, each simulation run lasted 10 ms "simulation time", with the results evaluated for the final 2 ms to eliminate the effect of the initial system and controller transients.

In each simulation, the rotor is sinusoidally displaced 50 microns from center at 1 kHz for both axes. The first harmonic coefficients of the sine and cosine terms of the Fourier series performed on the estimated displacement were used to determine magnitude and phase. This 2-term series was subtracted from the estimator data, and the RMS noise values were then determined for both axes.

In simulations involving failures, the current in the "actual" model and the applied voltage for the failed pole were set to zero. Neither the "simulation" model nor the controller was altered, however, in order to evaluate the performance of the simplest hardware configuration (one controller and bearing model used over a range of fault states). Table 1 lists the results of several illustrative simulations.

Figure 5 depicts the estimator output for case 5, where coils on either side of the $y-$axis coil are failed. Noticable features include a modest mean offset as well as some harmonic distortion most evident at the extrema of journal motion. This error is reflected in the increased RMS error figure of 10.0 microns for this run.

The results demonstrate that there is little decrease in estimator performance under all single-coil fault conditions and under several double-coil fault conditions.

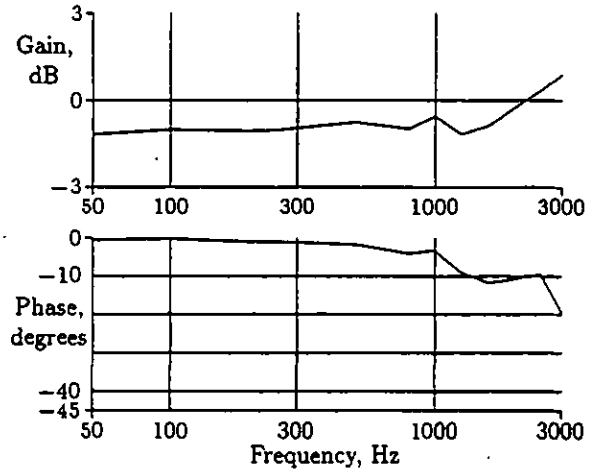

Figure 6: No-fault controller Bode plot at 50 micron input displacement magnitude

The worst performance under any single-coil fault condition is a magnitude error of 5.4% and phase lag difference of -1.1° of the no-fault estimated position values, with only a slight decrease in position accuracy for the double-coil fault scenario. While noise levels increased significantly under the various fault conditions, the high-frequency components of the noise can be removed with proper filtering in the controller which reflects the physical limitations of the actual system. Offset errors introduced by fault conditions might be removed by simply establishing the correlation between the error and the fault, assuming that this correlation is consistent.

Figure 6 presents the Bode plot for the no-fault case over a range of frequencies, all at an input displacement magnitude of 50 microns. This demonstrates that under normal operating conditions, the controller provides acceptable performance over the entire range of typical operating frequencies. Because the simulation contains no noise, the controller tracks the position past the filter cutoff frequency of 2kHz. With noise, the performance will begin to degrade near the cutoff frequency.

The geometric parameters for the bearing model were chosen to be consistent with the model developed in [5]. Better performance could be achieved with a geometry that increases the sensitivity of the filter output to displacements, such as decreasing the nominal gap length to increase the sensitivity of the inductance

to displacement. It follows that the self-sensing technique must often be matched with a suitable application. High sensing performance requires special bearing geometries that maximize the range of current slope magnitudes delivered by the filters. The greater sensitivity to displacement, the higher accuracy of sensed position.

Discrete position sensors will, in general, offer even higher signal-to-noise ratios than can be delivered by bearing geometries and materials optimized for self-sensing because they do not have to simultaneously satisfy the performance requirements of actuation and sensing, which are somewhat in conflict. Thus, for applications which require very tight rotor-bearing tolerances or very stiff suspensions, discrete position sensors may be required.

CONCLUSIONS AND FUTURE WORK

This paper has demonstrated that a self-sensing scheme can provide acceptable position accuracy and bandwidth under various fault conditions. Furthermore, it has examined the increase in noise and the loss of bandwidth under these fault conditions.

Of particular importance is the observation that a single estimator can suffice for wide range of fault scenarios. This is significant because the very high throughput requirements of the estimator (greater than 100 kHz) demand that it be implemented in analog circuitry. Consequently, it is advantageous to use a single controller for all fault states. The reasons include both space considerations as well as cost and complexity of implementing controller switching bardware: this is not a simple matter of software selection of a different algorithm depending on fault state.

Future work for the controller includes designing filters that reflect the fundamental physical limitations of the system. In the present development, the signals x, y, and g were treated as random variables for the purpose of controller construction. However, these signals have reasonably bounded spectra: these bounds can be explicitly acknowledged in synthesizing the controller. Additionally, the present development doesn't include a noise model for the signals z. As such, the controller attempts to extend the sensor bandwidth to an extent which is probably not feasible in physical hardware (experimental experience with the single magnet problem supports this.) Again, as in the case of the displacement signals, estimates of bounds on the noise spectra can be made and incorporated into the controller synthesis. This would be expected to achieve a suitable balance between estimator bandwidth and noise rejection.

In addition, application of this general methodology to tri-state switching amplifiers is viewed as a prerequisite to broad commercial application. There is no fundamental problem with applying this parameter estimation paradigm to tri-state amplifiers, but significant effort must be expended in determining the appropriate signal processing to best extract the current slope information which is nearly buried in sensing noise for these amplifiers.

Finally, as noted by Noh[7], magnetic saturation presents a substantial challenge to self-sensing magnetic bearings. The parameter estimation scheme provides a perfect hook into solving this problem because the embedded model can potentially be changed to include an approximation to the saturation nonlinearity, which should then allow the estimator to account for saturation. However, this poses numerous technical challenges including economical circuit implementation of the magnetic nonlinearities, appropriate identification methods, and the stability of the estimation network with this new plant whose gain would now be substantially nonlinear.

Experimental testing is initially planned for a rigid-rotor, two-bearing assembly which includes disturbance application while operating in the bearing non-saturation regime. Eventual testing will be performed into the saturation region under all types of amplifier fault conditions that are actuator tolerable.

REFERENCES

[1] Demarest, Kenneth R., *Engineering Electromagnetics.* Prentice Hall, Upper Saddle River, NJ, 1998.

[2] Green, M. and Limebeer, D. J. N., *Linear Robust Control,* Prentice Hall, Englewood Cliffs, NJ, 1995.

[3] Iannello, V., *Sensorless Position Detector for an Active Magnetic Bearing.* U.S. Patent pending. Application No. 08/138,217.

[4] Keith, F. J., Maslen, E. H., Humphris, R. R., and Williams, R. D., "Switching Power Amplifier Design for Magnetic Bearings," *Proceedings of the Second International Symposium on Magnetic Bearings,* Tokyo, Japan, July 12-14, 1990, pp. 211-218.

[5] Meeker, D. C., *Optimal Solutions to the Inverse Problem in Quadratic Magnetic Actuators.* Ph.D. Dissertation, University of Virginia, 1996.

[6] Mizuno, T., Bleuler, H., Gähler, C., Vischer, D., "Towards Practical Applications of Self-Sensing Magnetic Bearings," *Proceedings of the Third International Symposium an Magnetic Bearings.* Tokyo, Japan, August 1992.

[7] Noh, M. D., *Self-Sensing Magnetic Bearings Driven by a Switching Power Amplifier.* Ph.D. Dissertation, University of Virginia, 1996.

[8] Vischer, D., and Bleuler, H., "A New Approach to Sensorless and Voltage Controlled AMBs Based on Network Theory Concepts," *Proceedings of the Second International Symposium on Magnetic Bearings,* Tokyo, July 12-14, 1992, pp. 301-306.